UCRL-ID-141546

Field Validation of the NUFT Code for Subsurface Remediation by Soil Vapor Extraction

J.J. Nitao, S.A. Martins and M.N. Ridley

U.S. Department of Energy

Lawrence Livermore National Laboratory

September 23, 2000

DISCLAIMER

Work performed under the auspices of the U. S. Department of Energy by the University of California Lawrence Livermore National Laboratory under Contract W-7405-Eng-48.

Field Validation of the NUFT Code for Subsurface Remediation by Soil Vapor Extraction

John J. Nitao
Stanley A. Martins
Maureen N. Ridley
Lawrence Livermore National Laboratory

September 23, 2000

Field Validation of the NUFT Code for Subsurface Remediation by Soil Vapor Extraction

John J. Nitao
Geosciences and Environmental Technologies Division

Stanley A. Martins, Maureen N. Ridley
Environmental Restoration Division

September 23, 2000

Contents

Acknowledgements

This work was funded by the DOD/DOE Strategic Environmental Research and Development Program (SERDP) as part of a project directed by the U.S. Army Engineer Research and Development Center, Waterways Experiment Station (WES), Vicksburg, Mississippi. We would like to thank Dr. Mark Dortch at WES without whom this work would not have been possible. We would also like to thank the management of the LLNL Environmental Restoration Division for allowing us to present the data used in the report. Work performed at LLNL is under the auspices of the U.S. Department of Energy, under Contract W-7405-Eng-48.

1. Introduction

Soil vapor extraction (SVE) is a widely-used method for remediation of contaminants in the unsaturated, or vadose, zone. SVE removes volatile contaminants by extracting gases from the subsurface. The pressure gradients necessary to drive gas flow are limited by at most one atmosphere of vacuum. Therefore, a common adjunct to SVE is the injection of fresh air into the subsurface at a distance from the extraction wells in order to increase overall gas pressure gradients, and, hence, flow rates. SVE has also been used for saturated zone remediation by first pumping the water table down to expose free phase contaminants.

The selection of a vadose zone remediation method depends on a variety of site parameters. The type of contaminant is a major factor. Obviously, the selection of SVE as a method makes sense only for volatile contaminants since, otherwise, gas phase transport would be impossible. Bioventing is often a cost-effective candidate for contaminants that biodegrade easily in an aerobic environment, such as petroleum hydrocarbons. Bioventing shares some similarity to SVE, except that the flow rates are usually much lower. Whereas, the main goal of bioventing is to provide oxygen to the micro-organisms that break-down the contaminant; the main goal of SVE is physical removal.

Biodegration may be, for some contaminants, an important side benefit of SVE. However, bioventing and other forms of bioremediation are not considered to be effective for chlorinated vadose zone contaminants, such as trichloroethylene (TCE), which does not biodegrade readily in an aerobic environment. Soil excavation is a viable remediation method for the shallow spills where there are no existing important man-made structures. Otherwise, SVE is often the most appropriate and widely used remediation method for VOC's in the vadose zone.

2. Objectives

Lawrence Livermore National Laboratory (LLNL) is funded by the DOD/DOE Strategic Environmental Research and Development Program (SERDP) under the direction of the U.S. Army Engineer Research and Development Center, Vicksburg, Mississippi, in an effort to leverage and share expertise in subsurface contaminant remediation technology. This particular Project consists of validation of the NUFT code against field remediation data for SVE. The project involves demonstrating the performance of the NUFT code by comparing it to data from a well-characterized and evaluated SVE remediation site.

This particular project focuses on developing a validation of the NUFT code against SVE data from the Building 518 (B-518) site at the Lawrence Livermore

National Laboratory, Livermore, California. This site was selected because of its extensive site characterization and monitoring.

The processes modeled for SVE, the advective and diffusive gas transport of contaminants, is present in other remediation methods such as bioventing, air sparging, dyanmic steam stripping, and, therefore, the relevance of this study extends well beyond SVE as a model validation exercise.

3. Important Aspects of SVE Remediation

Factors Impacting SVE Effectiveness

The effectiveness of SVE hinges on several interelated site factors. The first major factor is the distribution of subsurface pneumatic properties. Air will tend to travel through flow paths of highest permeability, bypassing low permeability regions. Because these high-flow paths are well-flushed, the air in them will have lower contaminant concentrations than the surrounding regions. Contaminants in the tighter regions will travel primarily by molecular diffusion towards the high-flow paths.

The spatial location and distribution of contaminants is another major factor, especially in relationship to to the type of soil structure. As just mentioned, contaminants in the finer-grained soil will travel by diffusion towards high flow pathways in nearby coarser-grained "stringers." Because finer-grained soils tend to have a higher percentage of their pores filled with water, not only do they inhibit advection, but molecular diffusion as well.

This observation leads us to a third major factor: the soil moisture content and its distribution. High moisture content can significantly lower the gas phase permeability causing air to flow more readily through regions of low moisture content, such as sandy or gravelly sediments. Gas diffusion coefficients are also significantly lower in high moisture content materials. It is known that clayey soil zones will often be close to being saturated, even under semi-arid climatic conditions. The unsaturated properties of the soil is particularly important when considering remediation using saturated zone dewatering methods. A tight soil can take years to drain, making SVE of the saturated zone ineffectual.

Current Industry Remediation Design Practice

Of immediate interest to the engineer that is designing the SVE system are: (1) what is the necessary number of extraction and injection wells and their locations, and (2) what are their flow rates. Current common industry practice is the successive placement of wells in regions of high contaminant concentration until

most of the spill lies within the "radius of influence" of a well or of the combined well system. The radius of influence is determined by monitoring gas pressure at selected points during a pre-test period to find where "significant" pressure drop occurs. A difficulty with the approach is that pressure is not a good measure of flow. In fact, numerical modeling shows that both low and high flow areas can have almost identical magnitudes in pressure drop. This observation is supported by field measurements which often indicate nearly symmetrical pressure contours at highly heterogeneous sites.

Another subject of concern to the design engineer is the expected history of recovered contaminant mass because of his interest in the design of the surface collection facility. Related questions facing the engineer are the expected time to completion and the determination of whether remediation has been successful. These last two questions are not straight-forward because there is no minimum regulatory standard for contaminants in the vadose zone. Common industry practice is to deem the remediation to be successful when concentrations in the vapor extraction stream become "sufficiently low." The question remains as to what is "sufficiently low," and whether the extraction stream has passed through all zones of high contamination.

Use of Numerical Modeling

An integrated procedure incorporating numerical modeling, laboratory and field measurements overcomes many of the problems that have been posed. Modeling plays a valuable role in all stages of remediation: site characterization, remediation design, treatiblity demonstration, on-site monitoring, and closure.

Modelling is an important driver to determining what laboratory and field data are most relevant to answering key questions. Without modeling, resources may be inappropriately focused on obtaining the wrong type of data or on making improvements to the accuracy of measurements beyond that which is necessary. Modelling requires that the physical processes of the problem be, first, identified and conceptualized so that the proper analytical or numerical model is selected. This step helps understand the fundamental laws that govern processes whose constitutive coefficients are being measured. The required input parameters to the model must, next, be obtained. A checklist will determine which parameters are missing or which are site-specific that need to be measured or estimated. Once the model is ready, parameter sensitivity simulations, can be run to see the impact of the input parameters in order to determine their relative importance.

In the design of the remediation method, models can be run to determine the result of "what if" scenarios by varying the type of method and design parameters, such as number of wells, lateral location of wells, vertical location of well screens,

and extraction rates, to see their impact on contaminant removal.

Model results can be used as a benchmark – monitoring data that do not agree with model predictions is often an indication that site characterization must be revisited and the estimated initial mass or location of soil structures must be re-evaluated. In this way, modelling provides a basis for determining if initial site characterization was correct in light of ongoing data.

Example of the Impact of Numerical Modeling on Field Remediation

The benefits of numerical modeling was clearly demonstrated at a SVE site for the remediation of a large TCE spill near Livermore, California (Appendix H, Rueth et al., 1998). The modeling study identified stagnation regions where contaminants were not being flushed, and, therefore, where additional wells were needed in addition to those in the initial design. Modeling showed that a combination of cyclic pumping and the additional wells will shorten the estimated cleanup time of the intial design by 20 years. It was also found that higher SVE extractions did not reduce cleanup times, because the system relatively quickly reaches a state whereby removal is limited by diffusive, and not advective, flow.

4. NUFT Flow and Transport Code

General Description

NUFT (Non-isothermal Unsaturated-saturated Flow and Transport model) is a generalized multipurpose computer code for modeling multiphase fluid flow and multi-species reactive transport in porous media under both non-isothermal and isothermal conditions (Nitao, 1998a; 1998b). It solves the partial differential equations for the conservation of mass and energy. NUFT is an efficient and robust code that has been used to simulate a wide range of computationally demanding problems. NUFT consists of several modules described previously in a single source code instead of multiple source versions. Each module has its own set of simplifying assumptions so that the user can select the most physically appropriate mathematical module and computationally efficient numerical solution method. The model input format is user-friendly, flexible, and upwardly compatible.

USNT is one of NUFT modules (Nitao, 1998). It solves the multiphase flow and multi-species transport equations under non-isothermal conditions. Those transport equations may be coupled by both equilibrium-based and kinetics-based reactions, such as the first-order, sequentially first-order, Monod, and dual-substrate Monod reactions.

5. Model Validation Study: B-518, Lawrence Livermore National Laboratory

5.1. Site Description

Lawrence Livermore National Laboratory (LLNL) is an 800 acre research facility owned by the U.S. Department of Energy (DOE) and operated by the University of California. It is located approximately 40 miles east of San Francisco, California and 3 miles east of downtown Livermore (see Fig. 5.1). The groundwater systems under LLNL consists of a shallow system of heterogeneous alluvial deposits and and a deeper system of fluvial and lacustrine sediments. Annual average precipitation is around 14 in/y.

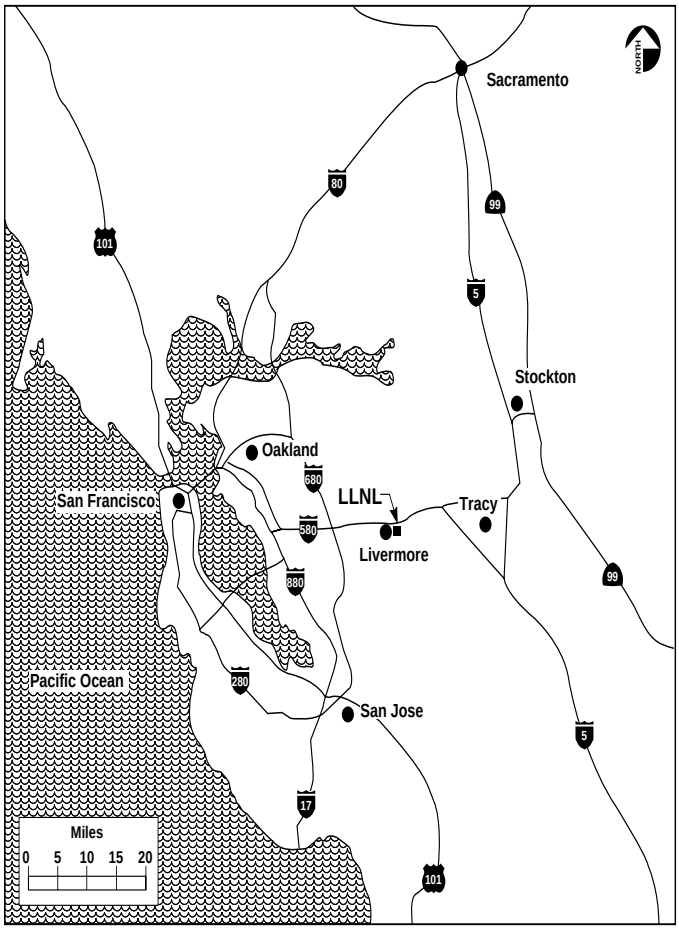

Figure 5.1. Location of the LLNL Livermore Site

B-518 was constructed in 1958 and has been used as a gas cylinder, solvent drum, and oil drum facility. Several sites around the former facility were identified by soil vapor surveys to have potentially high concentrations of VOC. Subsequent soil borings found VOC contamination with the highest concentration around the area of the subsequent location of well SIB-518-001 (Berg et al, 1994). The highest concentration was 6.3ppm soil concentration (kg VOC / kg total soil). Highest concentrations were in the first 50 ft from the ground surface which is in the vadose zone. The thickness of the vadose zone at this site is approximately 100 ft.

Twenty-five boreholes were initially drilled in the B-518 area. Three were monitor wells, one was a grounwater piezometer, and four were soil vapor extraction or vadose zone monitors (see Fig. 5.2).

These boreholes were drilled in 1984, 1989, and 1993. The lithologic and VOC data from selected boreholes is shown in Fig. 5.3. The total TCE mass was estimated by a spatial interpolation program (Dynamic Graphics Earth Vision) to be 22 kg.

5.2. The Pre-remediation Field Test

In 1993 a short field test was performed at B-518 to demonstrate the treatibility of the site. We will describe this test because the model in the validation study uses parameters calibrated from this test. The results of the test and corresponding model calculations were described in a Remedial Design Report (Berge et al., 1994). The numerical calculations were described in more detail in Vogele et al., 1996.

The test was performed in two steps. Solid vapor was extracted from SVB-518-201 for eight hours using a relatively constant extraction rate of 100 to 130 standard cubic feet per minute (scfm). The next day, soil vapor was extracted from the same well for five hours with extraction rates continually increasing from 1.9 to 86.2 scfm. Vapor samples were collected during both tests. Approximately 1.2 gal of TCE were removed.

Two types of soil distributions were used in the numerical model. A homogeneous model which has uniform hydrologic properties. A heterogeneous model which has a total of eleven different soil types. Heterogeneous soil distribution was based primarily on lithologic data, lithologic logs, and measurement of soil moisture which was found to correlate strongly with soil type (Lee, 1997). Distribution between data points were obtained using kriging. After the study was performed, Lee (1997) found that kriging does not adequately represent the true heterogeneity of the system.

Saturated and unsaturated hydrologic properties were based on measurements

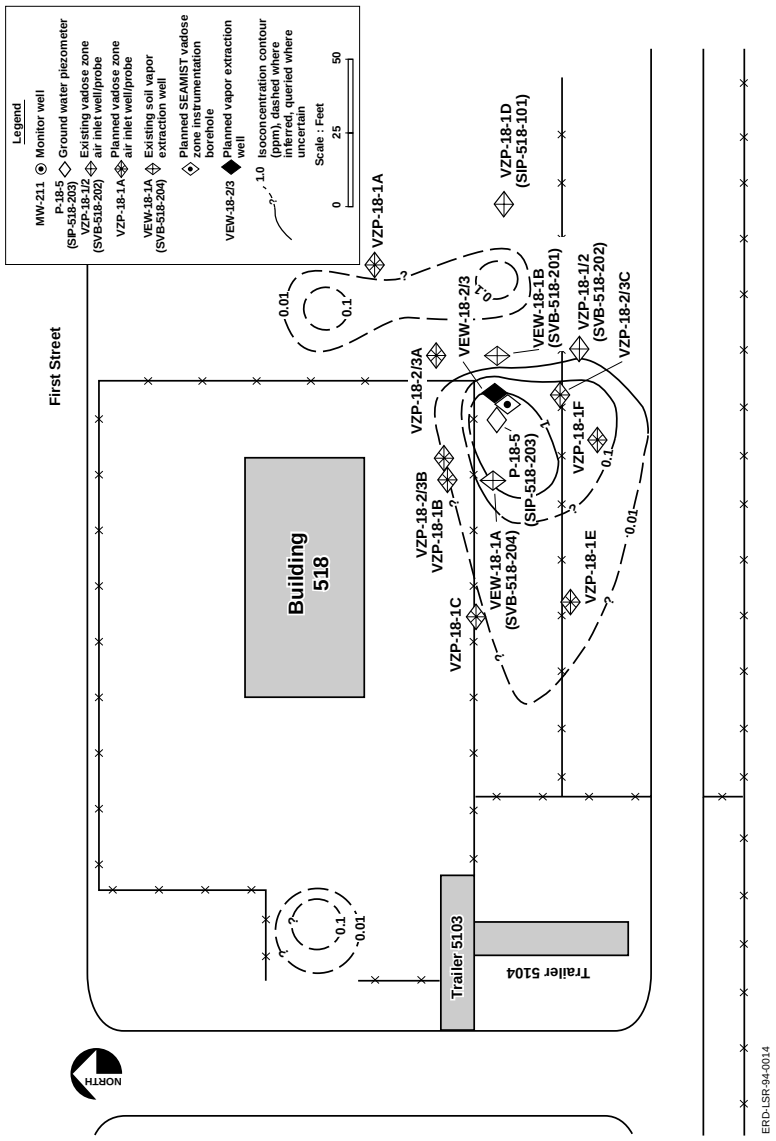

Figure 5.2. Vapor extraction well and vadose zone air inlet well/probe locations and total VOCs in soil at the 30-ft depth in the B-518 Area.

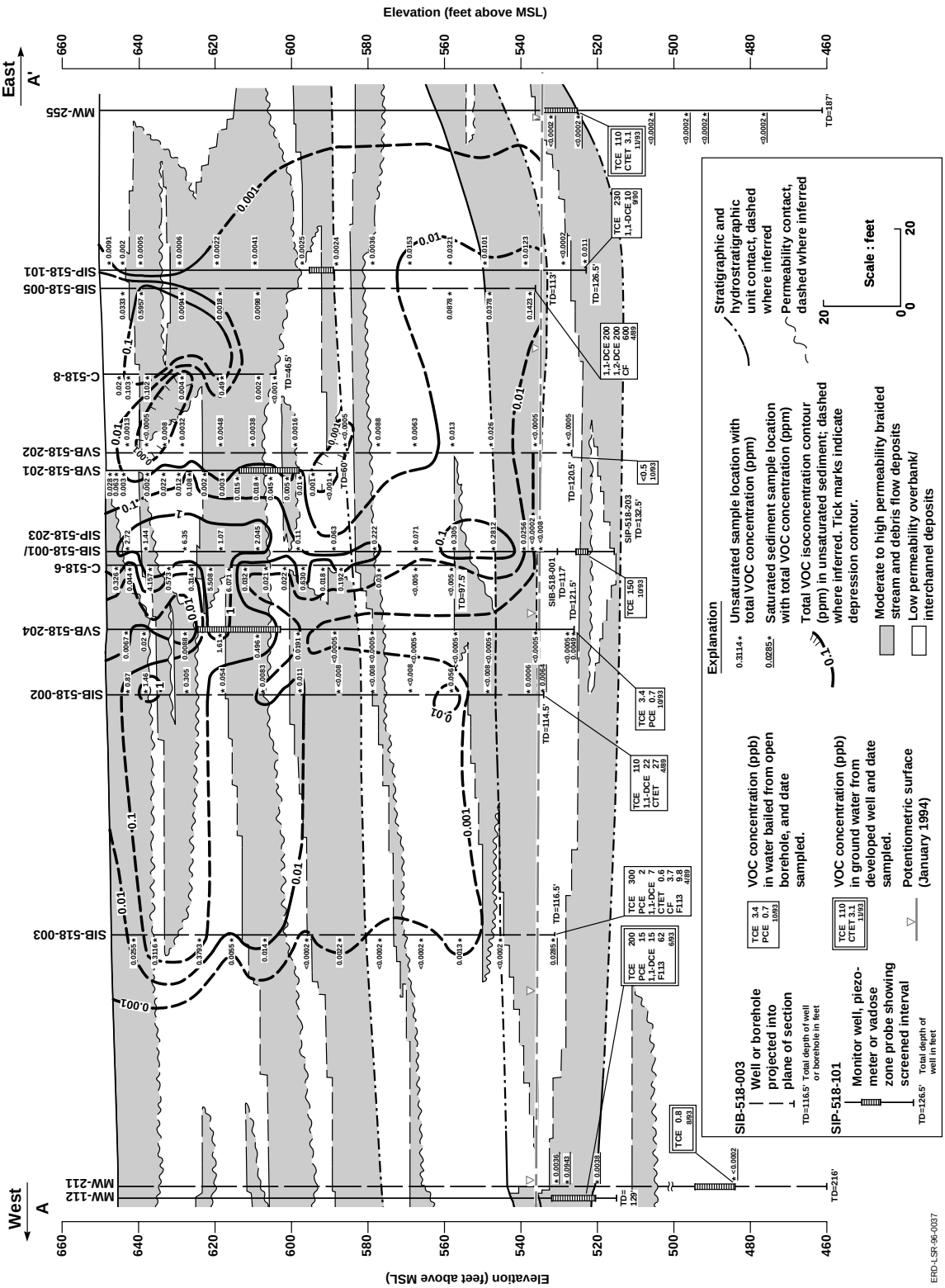

Figure 5.3. Hydrogeochemical cross section A-A' in the Building 518 Area.

at the Building 292 site at LLNL (Lee, 1997). Soil K_d values were typical values from other sites at LLNL. The initial relative soil concentration distribution were obtained by interpolation from well sample points.

Calibration of the mean permeability of both models was accomplished by applying the measured wellhead gas pressures to the model and comparing the predicted flow rates with those that were measured.

Using the calibrated mean permeability we then predicted the vapor concentration produced from the extraction stream. The total mass of the TCE was calibrated by comparing these concentrations with the measurement from the field test. The shape of the vapor concentration history curve agreed well with model predictions (see Fig. 5.4).

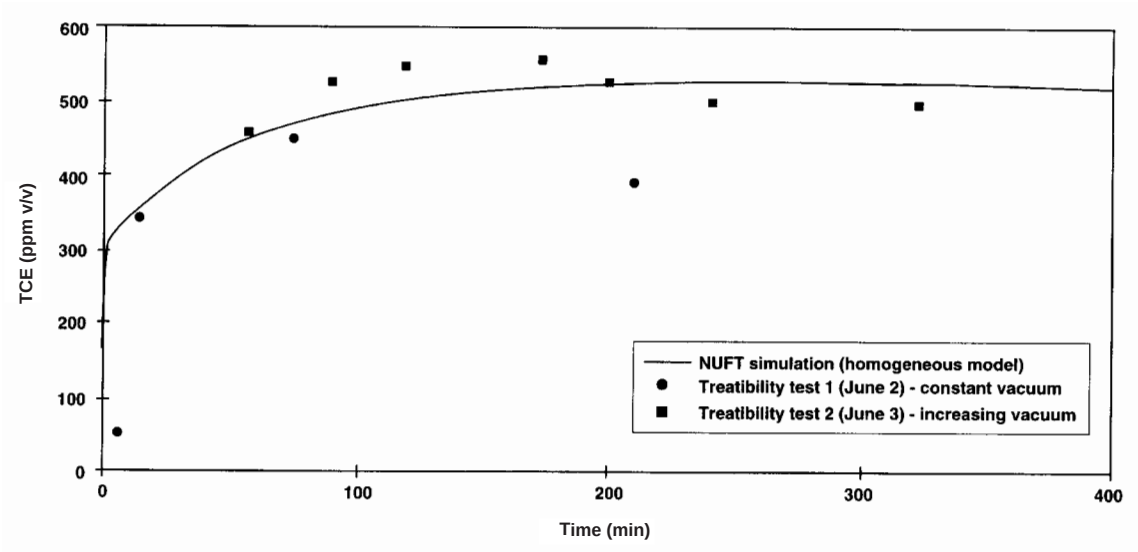

Figure 5.4. Comparison of SVE vapor concentrations from calibrated model with field data during the pre-remediation test.

It was found that the initial mass had to be increased up to five times the initial estimates using interpolation to match the concentration stream of the pre-test, possibily indicating that initial estimates were too low.

5.3. Model Validation using Data during Remediation

In September 1995, actual remediation of the site was begun using vapor extraction from borehole SVB-518-201. For model validation, an interesting question is how well does the model compare with the remediation data if we used parameters calibrated from the test of 1993.

We decided to focus on the first 19 months of extraction because after that period other injection and extraction wells began their operation, which would extend the problem domain beyond the intent of this study. Fig. 5.5 shows the history of the total gas extraction rate during this period. This flux history was input, after appropriate unit conversion, to the NUFT model in the form of a specified flux well condition.

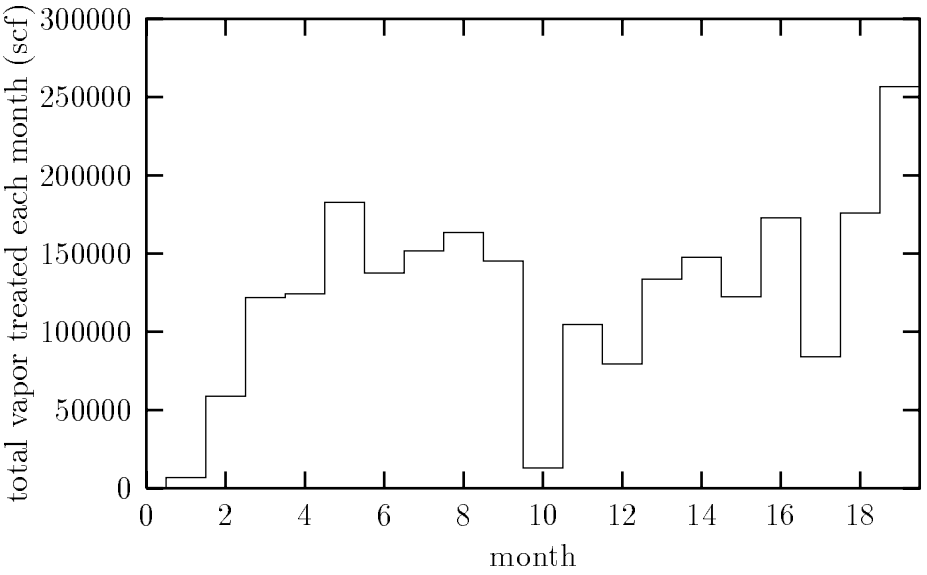

Figure 5.5. Total air-vapor extraction rate history of B-518-201.

The initial condition and hydrologic properties from the NUFT are the same as those calibrated from the pre-remediation field test in 1993. For that test, the two types of models from the study were used, one with homogeneous soil properties and one with interpolated-heterogeneous properties.

5.4. Conceptual Model

The subsurface flow and transport system is represented as a three-component system: water, air, and TCE. There are two fluid phases, gaseous and aqueous. Each one is composed of a mixture of the three components. Each component partitions into the two phases according to local equilibrium thermodynamics. The solid phase is nondeformable and nonreactive. However, TCE can adsorb onto its surfaces according to a linear adsorption isotherm. The temperature is assumed to be uniform in space and constant in time. The biodecay of TCE will be considered to be negligible in an aerobic environment. The governing

equations which mathematically describes the above conceptual model is presented in Appendix A.

The need for a two phase model with a mobile aqueous phase follows from the influence that infiltration rate has on the aqueous saturation which in turn affects the gas flow through the gas relative permeability. And, a mobile aqueous phase is needed to model the possible transport of contaminants through the vadose zone and down to the water table.

5.5. Model Geometry and Grid

The model geometry is cylindrically symmetric with the vapor extraction well (SVB-518-201) at the central vertical axis of symmetry. The upper boundary of the model is the atmosphere. The bottom boundary of the model domain extends to about 10 m below the water table. The vertical thickness of the vadose zone region is about 33.6 m. The lateral boundary extends to about 63 meters from the well.

The grid spatially discretizing the domain is shown in Fig. 5.6. The numerical values of the grid subdivisions are found in Appendix B. The extraction well is represented by the innermost column of cells which have a permeability much higher than the formation.

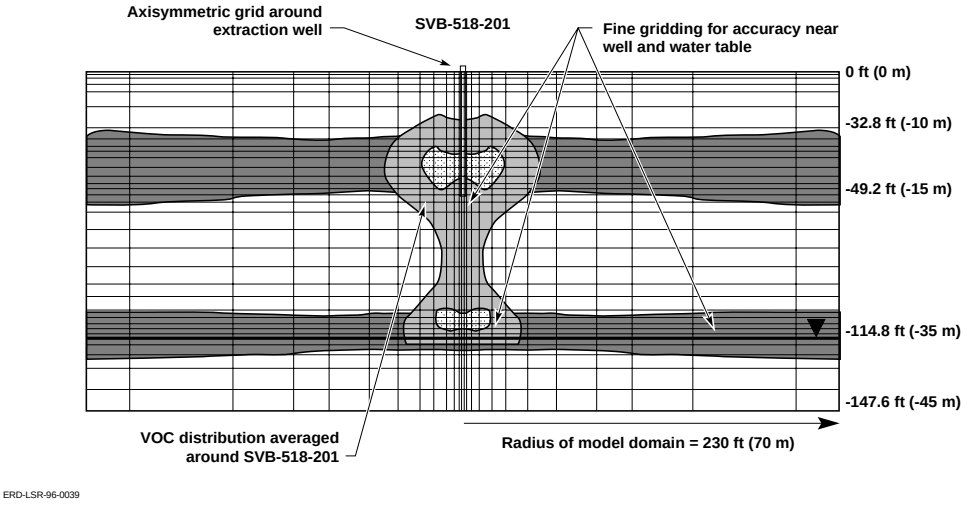

Figure 5.6. B-518 model grid.

5.6. Boundary conditions

The atmosphere is kept at constant pressure and humidity with zero TCE concentration. A constant infiltration flux equivalent to 1.33 in/yr, which is equal to 10% of the mean precipitation, is imposed a short distance below the ground surface. Gas and liquid pressures at the lateral boundaries of the model are kept fixed at their initial values calculated by the initial steady-state run as explained in the next subsection. The gas extraction flux history at the well is set to that measured in the field. The bottom of the model is at no-flow conditions. Aquifer pressure support comes from the lateral aquifer boundary which is kept at constant pressure head.

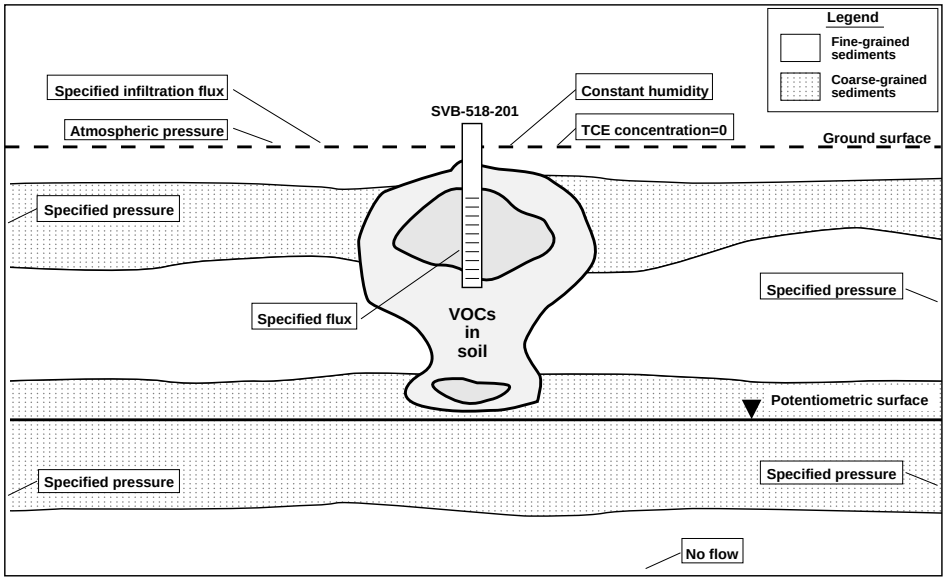

Figure 5.7. Boundary conditions for the B-518 model.

5.7. Initial conditions

The initial pressures and saturation of the model were obtained by performing a run with the above boundary conditions except there is no well imposed and the outer boundaries are not kept fixed. The bottom boundary of the model is kept fixed at the hydrostatic pressure of the approximate desired depth below the water table. It is important that there are enough model layers present that are saturated so that the bottom layer does not become unsaturated during the initialization run.

The initialization run is stopped when there are no longer significant changes in the solution variables (pressure, saturations, concentrations), indicating that steady-state has been reached. The vertical distributions in pressure and saturation at the end of the initialization run are used as initial conditions by the main simulation run. The initial aqueous saturation profile that is used is shown in Fig. 5.8.

Using an initialization run to obtain steady-state conditions is particularly important for simulations where gas flow is a dominant transport mechanism. Because of the low viscosity of gases, any slight disequilibrium in gas pressures at the boundary conditions may lead to significant false gas currents.

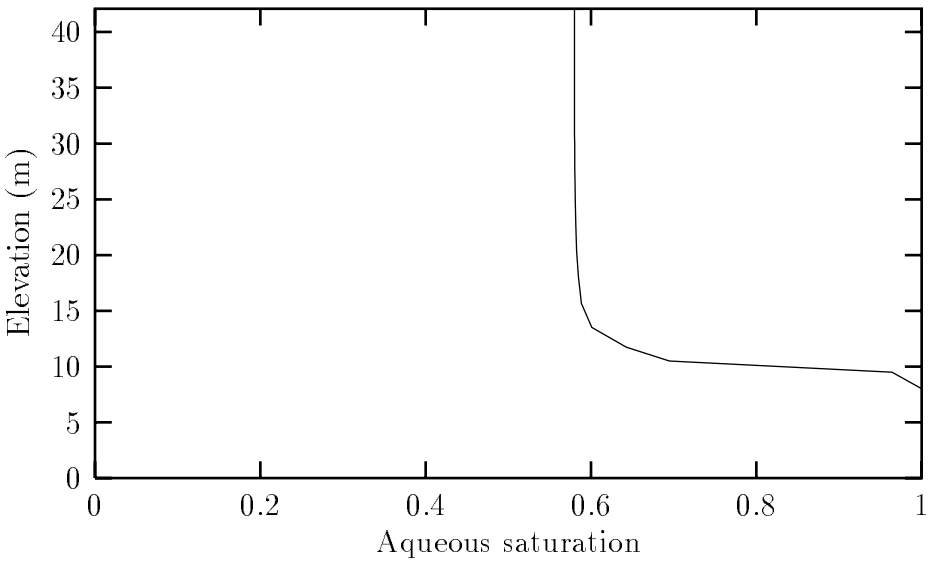

Figure 5.8. Initial vertical saturation distribution.

The total soil concentration distribution of TCE (kg TCE / kg bulk soil) is obtained from spatial interpolation between well sample points using kriging. Because the model is cylindrically symmetric, the concentrations are, then, volume-averaged over cells in the angle around the central well axis. These concentration values, after the model internally converts them to aqueous mole fractions, are used as initial conditions for the TCE concentrations.

5.8. Hydrologic Properties

The material used in the homogeneous model is for a sandy-silt sediment obtained from a borehole at the Building 292 site at LLNL. It's measured hydrologic properties are given in Table 5.1.

Table 5.1. Sandy-silt material properties

porosity, ϕ	0.28,
saturated permeability, K	1.196×10^{-12} m^2,
bulk soil density, ρ_b	2.6×10^3 kg/m^3,
adsorption coefficient $\rho_b K_d/\phi$	2.0,
matric suction potential, p_{cap}	table, see Fig. 5.9,
van Genuchten parameter, m	0.192,
residual aqueous saturation	0.242,
residual gas saturation	0.10,
tortuosity factor, τ_α	Millington correlation, $\tau_\alpha = S_\alpha^{7/3}\phi^{1/3}$, $\alpha = \ell, g$.

For the matric suction potential, linear interpolation between laboratory data points obtained from the pressure cell method is used (see Fig. 5.9). The van Genuchten parameter m is defined in Appendix A. It was obtained by fitting the matric suction curve.

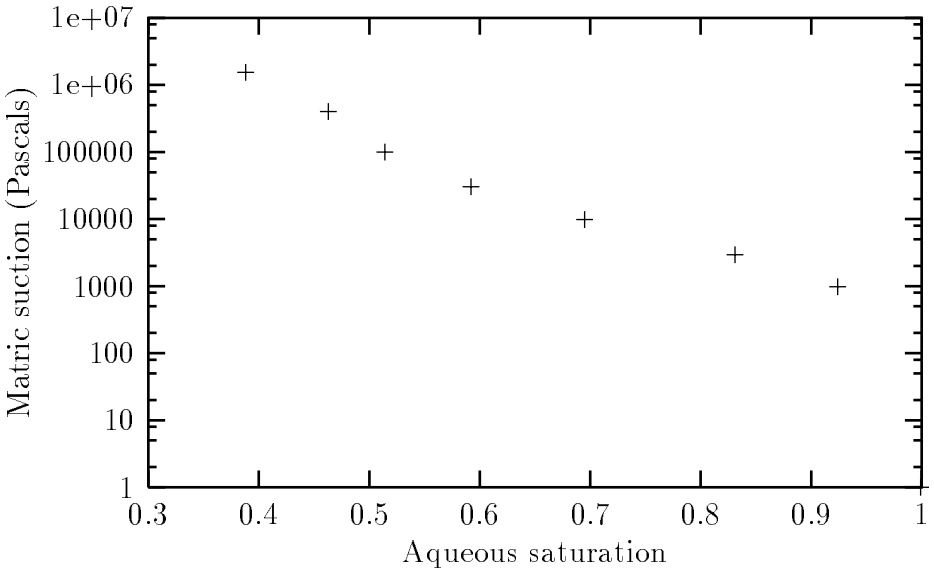

Figure 5.9. Matric suction curve for silty-sand material.

5.9. Model Results

The cumulative TCE production from the extraction well as measured in the field for the first 19 months of extraction is shown in Figure 5.10. Also shown is the

predicted model results for the homogeneous model calibrated during the 1993 pre-test. Considering the uncertainties involved in field characterization there is a reasonable match. Increasing the initial total mass which was estimated in the 1993 test by 10% gives even a better match, as shown in the figure.

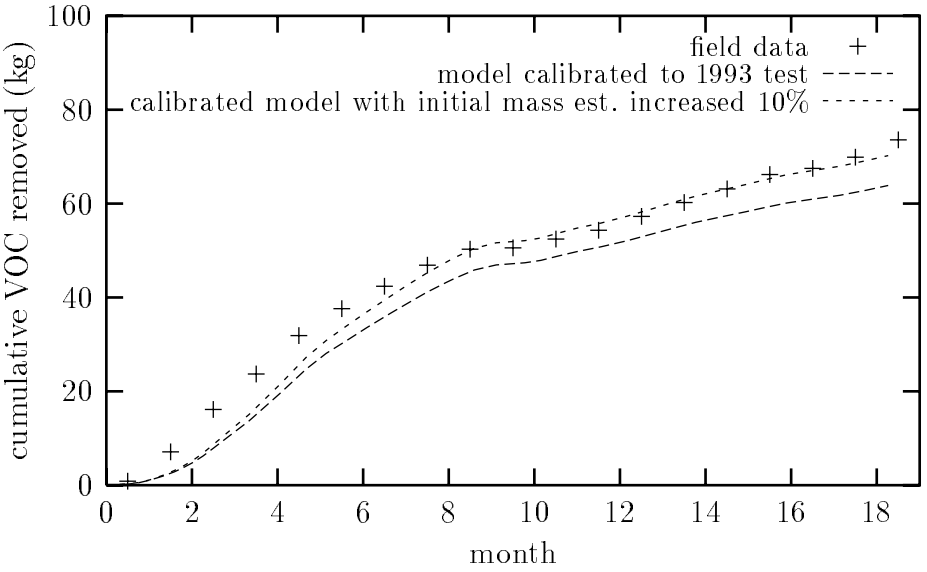

Figure 5.10. Comparison of TCE vapor extraction rate history with model predictions.

The results for the heterogeneous model is not shown because the initial mass obtained by calibrating the model during the 1993 test is much less than that produced during the first 19 months of extraction. The heterogeneous model required two times the 22kg estimate which was obtained by interpolation of well sample points. The homogeneous model required five times greater.

The lack of agreement for the heterogeneous case may be due to the extreme lateral smearing of soil types caused by the spatial interpolation method. This promotes extreme lateral flow which means that relatively low initial contaminant masses were sufficient to produce the concentrations observed in the 1993 test. However, beyond the short time frame (2 days) of the test the contaminants become flushed and the concentrations are too low to match the remediation data. This hypothesis is reinforced by the work of Lee (1997) who found that stochastic field generation of hydrologic properties is a much better method than interpolation methods because it does not laterally smear soil types.

Note that our site has no observed free product. One can argue that the presence of large amounts of relatively immobile free product makes model validation of SVE less challenging since the volatile contaminant concentration in

the vapor, and therefore in the produced stream, will stay close to the saturated thermodynamic value, and will not be strongly affected by flow and transport processes.

6. Conclusions

Although the main goal of this study is model validation agains SVE, we have also shown an example of how a numerical model can be calibrated against a short field extraction test to improve initial mass estimates of a volatile contaminant. Using a homogeneous model is more likely to give conservative estimates as opposed to a heterogeneous model using simple spatial interpolation between wells. Even more preferable is the use of stochastic interpolation methods.

Using the same homogeneous model that was calibrated against the two-day treatibility test in 1993 at B-518, we obtained very good agreement with the produced stream obtained during the first 19 months of remediation using SVE from the same well.

References

Berg, L.L., Dresen, M.D., Folsom, E.N., Bainer, R.W., Gelinas, R.J., Nichols, E.M., Bishop, D.J., Ziagos, J.P. (eds.) 1994, Remedial Design Report No. 6 for the Building 518 Vapor Treatment Facility Lawrence Livermore National Laboratory Livermore Site, Lawrence Livermore National Laboratory, Livermore, CA, Report no. UCRL-AR-115997.

Lee, Kenrick, 1997, Analysis of Vadose Zone Tritium Transport from an Underground Storage Tank Release Using Numerical Modeling and Geostatistics, Ph.D. thesis, University of California, Berkeley. (also Lawrence Livermore National Laboratory Report no. UCRL-LR-128840.).

Meyer, C.A., McClintock, R.B., Silvestri, G.J., (1968) *Thermodynamic and Transport Properties of Steam,* second edition, Amer. Soc. Mech. Eng.. N.Y.

Nitao, J. J., 1998, Reference Manual for the NUFT Flow and Transport code, Version 2.0, Lawrence Livermore National Laboratory, Livermore, CA Report no. UCRL-MA-130651.

Nitao, J. J., 1998, User's Manual for USNT module of the NUFT code, Version 2.0, Lawrence Livermore National Laboratory, Livermore, CA, Report no. UCRL-MA-130653.

Parker, J.C., Lenhard, R.J., Kuppusamy, T. (1987), A Parametric Model for Constitutive Properties Governing Multiphase Flow in Porous Media, *Water Resour. Res.,* vol. 23, no. 4, 618-624.

Rueth, L. S., Ferry, R. A., Green-Horner, L. K., DeLorenzo, T. H., 1998, Remedial Design document for the General Services Area Operable Unit treatment facilities, Lawrence Livermore National Laboratory, Site 300, Lawrence Livermore National Laboratory, Livermore, CA Report no. UCRL-AR-127465.

Vogele, T.J., Kulreshta, A., Nitao, J.J., Lee, K. (1996), Simulation of Soil Vapor Extraction at Building 518 Lawrence Livermore National Laboratory Site, Report no. UCRL-AR-124995.

A. Appendix A: Governing Equations Used in Modeling the SVE Problem

In this study the USNT module was configured by the options set in the input file to solve a three component system containing air (a), water (w), and volatile contaminant (c) in a system containing aqueous (ℓ) and gaseous (g) phases. The code solves the three mass balance equations for these components. These equations are partial differential equations that include transport by advection and molecular diffusion and the equilibrium partitioning of components between the fluid phases.

We will use the convention that subscripts will be used for fluid phases (ℓ or g) or the solid phase and superscripts (w, a, c) will refer to components.

The mass balance equations are

$$\begin{aligned}\frac{\partial}{\partial t}\phi\left(\rho_\ell X_\ell^w S_\ell + \rho_g X_g^w S_g\right) = \\ -\nabla\cdot\phi\left(\rho_\ell X_\ell^w S_\ell \boldsymbol{V}_\ell + \rho_g X_g^w S_g \boldsymbol{V}_g\right) \\ +\nabla\cdot\phi\left(\rho_\ell S_\ell \tau_\ell \mathcal{D}_\ell^w \nabla X_\ell^w + \rho_g S_g \tau_g \mathcal{D}_g^w \nabla X_g^w\right) + q^w,\end{aligned} \tag{A.1}$$

$$\begin{aligned}\frac{\partial}{\partial t}\phi\left(\rho_\ell X_\ell^a S_\ell + \rho_g X_g^a S_g\right) = \\ -\nabla\cdot\phi\left(\rho_\ell X_\ell^a S_\ell \boldsymbol{V}_\ell + \rho_g X_g^a S_g \boldsymbol{V}_g\right) \\ +\nabla\cdot\phi\left(\rho_\ell S_\ell \tau_\ell \mathcal{D}_\ell^a \nabla X_\ell^a + \rho_g S_g \tau_g \mathcal{D}_g^a \nabla X_g^a\right) + q^a,\end{aligned} \tag{A.2}$$

$$\frac{\partial}{\partial t}\phi\left(\rho_\ell X_\ell^c (S_\ell + \rho_b K_d^c/\phi) + \rho_g X_g^c S_g\right) + \lambda_\ell^c \phi \rho_\ell X_\ell^c (S_\ell + \rho_b K_d^c/\phi) =$$

$$-\nabla\cdot\phi\left(\rho_\ell X_\ell^c S_\ell \boldsymbol{V}_\ell + \rho_g X_g^c S_g \boldsymbol{V}_g\right)$$
$$+\nabla\cdot\phi\left(\rho_\ell S_\ell \tau_\ell \mathcal{D}_\ell^c \nabla X_\ell^c + \rho_g S_g \tau_g \mathcal{D}_g^c \nabla X_g^c\right) + q^c, \qquad \text{(A.3)}$$

ρ_α	mass density of the α fluid phase,
ρ_b	bulk soil mass density,
τ_α	tortuosity factor of the α fluid phase,
ϕ	porosity,
$\mathcal{D}_\alpha^\gamma$	free diffusion coefficient of the γ component in the α fluid phase,
S_α	saturation the α fluid phase,
X_α^γ	mass fraction of the γ component in the α fluid phase,
$\boldsymbol{V}_\alpha$	mass-weighted velocity of the α fluid phase,
q^γ	source term of the γ-component.
λ_ℓ^c	decay constant of contaminant component in the aqueous phase (taken to be zero in this study)

The fluid velocities are given by the multiphase version of Darcy's law,

$$\phi S_\ell \mathbf{V}_\ell = -\frac{K k_{r\ell}(S_\ell)}{\mu_\ell}\left(\nabla p_\ell + \rho_\ell g \nabla z\right), \qquad \text{(A.4)}$$

$$\phi S_g \mathbf{V}_g = -\frac{K k_{rg}(S_\ell)}{\mu_g}\left(\nabla p_g + \rho_g g \nabla z\right). \qquad \text{(A.5)}$$

Here, K is the saturated intrinsic permeability, k_{rg} and $k_{r\ell}$ are the relative permeability functions, μ_g and μ_ℓ are fluid viscosities, g is local gravitational acceleration, and z is the elevation coordinate.

The phase pressures, p_ℓ and p_g, in the above equations obey the relationship

$$p_g - p_\ell = p_c(S_\ell), \qquad \text{(A.6)}$$

where $p_c(S_\ell)$ is the capillary pressure.

In the simulations described in this report, tables of $p_c(S_\ell)$ versus S_ℓ whose values were measured on the laboratory using the pressure cell method. For the relative permeabilities $k_{r\ell}$ and k_{rg} we used the two-phase extension to van Genuchten's method based on Parker et al. (1987). The necessary parameters were obtained by fitting the van Genuchten capillary pressure function to the laboratory measurements of capillary pressure. The aqueous phase relative permeability function that was used is

$$k_{r\ell} = S_{e\ell}^{1/2}\left[1 - (1 - S_{e\ell}^{1/m})^m\right]^2, \qquad \text{(A.7)}$$

where $S_{e\ell} = (S_\ell - S_{r\ell})/(S_{\ell max} - S_{r\ell})$. The gas phase relative permeability function is

$$k_{rg} = S_{eg}^{1/2}\left[1 - (1 - S_{eg})^{1/m})\right]^{2m}, \tag{A.8}$$

where $S_{eg} = (S_g - S_{rg})/(1 - S_{rg})$. Here, $S_{r\ell}$ and S_{rg} are the residual aqueous and gas phase saturations, and $S_{\ell max}$ is the maximum aqueous phase saturation.

Although mass fractions appear in the balance equations, it is more convenient to use mole fractions as unknowns. The mass fractions can be expressed in terms of mole fractions by the relationships,

$$X_\alpha^w = n_\alpha^w M^w/(n_\alpha^w M^w + n_\alpha^a M^a + n_\alpha^c M^c), \tag{A.9}$$

$$X_\alpha^a = n_\alpha^a M^a/(n_\alpha^w M^w + n_\alpha^a M^a + n_\alpha^c M^c), \tag{A.10}$$

$$X_\alpha^c = n_\alpha^c M^c/(n_\alpha^w M^w + n_\alpha^a M^a + n_\alpha^c M^c), \tag{A.11}$$

where M^w, M^a, and M^c are the molecular weights of the three components, and $\alpha = \ell, g$.

Assuming local thermodynamic equilibrium, the inter-phase partitioning relationships are

$$n_g^w/n_\ell^w = \mathcal{K}_{g,\ell}^w \tag{A.12}$$

$$n_g^a/n_\ell^a = \mathcal{K}_{g,\ell}^a \tag{A.13}$$

$$n_g^c/n_\ell^c = \mathcal{K}_{g,\ell}^c \tag{A.14}$$

where n_α^γ is the mole fraction of the γ-component in the α-phase and the $\mathcal{K}_{\ell,g}^\gamma$ is "equilibrium constant" of the γ-component, a function of pressure and temperature.

The mole fractions obey the following constraints

$$n_\ell^w + n_\ell^a + n_\ell^c = 1, \tag{A.15}$$

$$n_g^w + n_g^a + n_g^c = 1. \tag{A.16}$$

Assuming unit fugacity coefficients for the gaseous components we have

$$n_g^w = p_g^w/p_g, \quad n_g^a = p_g^a/p_g, \quad n_g^c = p_g^c/p_g, \tag{A.17}$$

where p_g^γ is the partial pressure of the γ component and p_g is the total gas pressure. Dalton's law, $p_g^w + p_g^a + p_g^c = p_g$, guarantees that the constraint $n_g^w + n_g^a + n_g^c = 1$ is satisfied. We use Henry's law for the air and contaminants, which considered as dissolved components,

$$n_\ell^a = H^a p_g^a, \quad n_\ell^c = H^c p_g^c, \tag{A.18}$$

where H^a and H^c are equal to the usual Henry's constant with the proper unit conversion. From (A.17) and (A.18) we obtain

$$n_g^a/n_\ell^a = 1/(p_g H^a), \qquad n_g^c/n_\ell^c = 1/(p_g H^c), \tag{A.19}$$

and, hence,

$$\mathcal{K}_{g,\ell}^a = 1/(p_g H^a), \qquad \mathcal{K}_{g,\ell}^c = 1/(p_g H^c). \tag{A.20}$$

For the water component, again assuming unit fugacity coefficient, we have

$$n_g^w = p_g^w/p_g. \tag{A.21}$$

Assuming Raoult's law, for a water-air system, we have

$$n_g^w = n_\ell^w p_g^w/p_g, \tag{A.22}$$

or

$$n_g^w/n_\ell^w = p_g^w/p_g. \tag{A.23}$$

In a porous medium, from Kelvin's law we have

$$p_g^w = p_{sat}(T)\exp(-\psi^w/\hat{\rho}^w M^w RT) \tag{A.24}$$

where $\psi(S_\ell)$ is the matric potential, $\hat{\rho}^w$ is the partial molar density of water, and $p_{sat}(T)$ is the saturated vapor pressure, obtainable from steam tables.

Hence, the equilibrium constant for water is given by

$$\mathcal{K}_{g,\ell}^w = p_{sat}(T)\exp(-\psi^w M^w/\rho^w RT)/p_g. \tag{A.25}$$

The model evaluates $p_{sat}(T)$ and other steam table quantities using internal tables which are generated using widely-accepted and highly accurate correlations (Meyer et al., 1968).

The model has various options for computing the mass density of fluid phases. Since aqueous solutes are dilute we used the steam table value for pure water. For the gas phase we used a modified ideal gas law

$$\rho_g = \rho^{wv}(p_g, T) + (1 - n_g^w)p_g/m_g RT, \tag{A.26}$$

where $\rho^{wv}(p_g, T)$ is the pure water vapor density computed from the steam tables, m_g is the number of moles per mass of gas phase, R is the gas constant, and T is absolute temperature.

The partial differential equations are discretized in time and space using the finite-volume method. Combined with the other equations that were given, the results set of nonlinear equations must be solved iteratively.

A complication in the solution procedure is that the unknowns for each computational cell must be switched if a fluid phase disappears or reappears. For example, if a cell initially has both aqueous and gaseous phases and but subsequently the aqueous phase disappears due to drying, the concentrations in the aqueous phase become undefined and the partitioning relationships no longer hold. The concentrations of the components in the gas phase must be used as unknowns. If later the aqueous phase returns through incoming flow of water, the partitioning relationships apply and either aqueous or gaseous saturation replaces one of the concentrations in the gaseous phase. For the model configured in the input file the following "primary variables" are used,

Case 1. two-phase conditions ($S_\ell > 0$, $S_g > 0$):	p_g, S_ℓ, n_ℓ^c,
Case 2. completely-dry conditions ($S_\ell = 0$, $S_g = 1$):	p_g, n_g^a, n_g^c,
Case 3. saturated conditions ($S_\ell = 1$, $S_g = 0$):	p_ℓ, n_ℓ^a, n_ℓ^c.

B. Appendix B: Annotated NUFT Input File for the SVE Problem

```
(usnt  ;; name of NUFT module

  (title "*B518* homogeneous case") ;; run title

  (modelname flow);; arbitrary name of model

  ;; stopping time is 42 months
  (tstop 42M)
  ;; initial time
  (time 0.0)
  ;; initial time step is 1 minute
  (dt 1m)

  ;; absolute time step tolerance
  (tolerdt (P 1.0e5)(S 0.3)(C 0.3)(C.TCE 3.e-7))

  ;; relative time step tolerance
  (reltolerdt (P 0.4)(S 0.0)(C 0.3)(C.TCE 0.1))

  ;; absolute NR conv. tolerance
  (tolerconv (P 100.)(S 0.005)(C 0.005)(C.TCE 1.e-8))

  ;; relative NR conv. tolerance
  (reltolerconv (P 0.005)(S 0.01)(C 0.0)(C.TCE 1e-3))

  ;; configure balance equations for components and fluid phases
```

```
(init-eqts
  (components water air TCE);; TCE conc set to zero for flow run
  (phases liquid gas);; no TCE free product
  (wetting-phase liquid);; most wetting phase
  (primary-phase gas);; phase w.r.t. which all fluid pressures
  ;; will be defined using capillary
  ;; relationship
  (isothermal);; constant temperature model
  ) ;; end init-eqts

;; set linear solver input parameters
;; use preconditioned conjugate gradient method
;; with incomplete LU (ILU) preconditioning
(linear-solver pcg)
(pcg-parameters  (precond ilu) (north 20) (toler 1.e-5)
  (itermax 100)
  ) ;; end pcg-parameters
;; degree of fill for ILU preconditioning
(ilu-degree 0)

;; set output formats
(output

  ;; output TCE flux from well
  (srcflux
    (comp TCE) (name well)
    (file-ext ".TCE.flx")
    (outtimes *)
    ) ;; end srcflux

  ;; output cumulative TCE flux from well
  (srcflux
    (comp TCE) (name well)
    (file-ext ".TCE.cum")
    (cumulative)
    (outtimes *)
    ) ;; end srcflux

  ) ;; end output

;; set material properties
(rocktab

  ;; pseudo material type for atmosphere above ground surface
  (ATM (porosity  0.99) (solid-density 2.6e3)
    (Kd
      (TCE 0.0);; conservative tracer
      (air 0.0)
```

```
    (water 0.0))
  (K0 2.e-10)(K1 0.)(K2 0.) ;; 1 order of mag. > highest PM perm
  (pc (liquid   0.0)) ;; non-porous medium whose phase pressures are equal
  (kr  (gas 1.0) (liquid 0.0))
  (tort (liquid 0.0)(gas 1.0));;
  ) ;; end ATM

;; impermeable pseudo soil type for inactive elements in well
(WEL (porosity  0.99)  (solid-density 2.6e3)
  (Kd
    (TCE 0.0);; conservative tracer
    (air 0.0)
    (water 0.0))
  (K0 0.)(K1 0.)(K2 0.)
  (pc (liquid   0.0))
  (kr (gas 0.0)(liquid 0.0))
  (tort (liquid 0.0)(gas 0.0))
  ) ;; end WEL

;; pseudo soil type for vapor extraction well screen
(SCR (porosity  0.99)  (solid-density 2.6e3)
  (Kd
    (TCE 0.0);; conservative tracer
    (air 0.0)
    (water 0.0))
  (K0 2.e-11)(K1 0.)(K2 0.);; 1 order of mag > highest perm
  (pc (liquid   0.0))
  (kr (gas krLinear (Sr 0.0))(liquid krLinear (Sr 0.0)))
  (tort (liquid 0.0)(gas 0.0))
  ) ;; end SCR

;; sandy-silt sediment, sample U-292-015-15.3U
(san1
  (porosity  0.28)
  (solid-density 2.6e3)
  ;; actually equal to rhoB * Kd / phi = Rd - 1.0
  (Kd
    (TCE 2.0) ;; equivalent to sat. retardation factor of 1+2.0 = 3.0
    (air 0.0)
    (water 0.0))
  ;; saturated permeability
  (K0 1.196e-12)(K1 0.)(K2 0.)
  ;; table of capillary pressure vs. aqueous saturation
  (pc (liquid pcTable (table
                       0.0     5.88e6
                       .388  1.537e6
                       .463  400101
                       .514  100050
```

```
                        .592   30309
                        .695    9809
                        .831    2943
                        .924     981
                        1.0      0.0
                        ) ;; end table
          ) ;; end liquid
      ) ;; end pc
    ;; two-phase van Genuchten relative permeabilities
    (kr (gas krlVanGen  (m 0.192) (Sr .10)  (Sa .96)))
        (liquid krlVanGen (m 0.192) (Sr .242) (Sa .96)))
    ;; Millington tortuosity factor
    (tort
        (liquid  Millington (Sr 0.242))
        (gas Millington (Sr 0.10)))
    ) ;; end san1

  ) ;; end rocktab

;; fluid phase properties
(phaseprop
  ;; aqueous phase properties
  (liquid
    (rhoP rhoPLiqWat)
    (viscosity visLiqWat)
    )
  ;; gaseous phase properties
  (gas
    (rhoP rhoPZFacStm)
    (viscosity visGasAirWat)
    )
  );; end phaseprop

;; component properties
(compprop
  ;; water component properties
  (water
    ;; molecular weight (g/mol)
    (intrinsic (MoleWt 18.))
    ;; water vapor properties
    (gas    (Keq KeqWatVapor)
            (freeDiffusivity 7.7e-6)
      )
    ;; properties when in an aqueous phase
    (liquid (freeDiffusivity 1.0e-9);; approximate value
      (Keq 1.0);; since liquid is reference phase
      (rhoC rhoCLiqWat)
      )
```

```
    )
  ;; air component properties
  (air
    (intrinsic (MoleWt 29.))
    (gas    (Keq KeqStd (C 0.973e11)(D 0.0))
      (freeDiffusivity 7.7e-6))
    (liquid (freeDiffusivity 1.0e-9)
      (Keq 1.0))
    ) ;; end air

  ;; TCE component properties
  (TCE
    (intrinsic (MoleWt 131.5))
    (gas    (Keq KeqTCESolute)
      (freeDiffusivity 7.7e-6))
    (liquid
      (freeDiffusivity 1.0e-9)  (Keq 1.0)
      (rhoC rhoCLiqWat));; approximation for dilute solution
    ) ;; end TCE

  );;end compprop

(generic
  (T 12.5);; constant temperature in degrees C
  ) ;; end generic

;; set boundary conditions
(bctab
  ;; atmospheric boundary conditions are kept fixed at specified
  ;; conditions
  (atmos
    (range "T*")
    (basephase gas)
    (tables
      (S.liquid 0.0 0.0 1.e20 0.0)
      (C.air 0.0 0.995 1.e20 0.995)
      (C.TCE 0.0 0.00  1.e20 0.00)
      (P 0.0 1.e5 1.e20 1.e5)
      )
    ) ;; end atmos

  ;; outer boundary is kept at fixed at initial conditions
  (outer-bnd (range "B*") (clamped))

  ) ;; end bctab

;; source terms
(srctab
```

```
;; source terms at atl well elements
(phaseflux
  ;; name of source term set, for srcflux output option
  (name well)
  ;; name of phase being extracted
  (phase gas)
  ;; allocate total flux in the table given below
  ;; over cells relative to their volume
  (allocate-by-volume)
  ;;  1/(30*60*24)  factor of 30 already present
  (allocate-by-element ("*" 2.31e-5))
  ;; range of elements that will be extracted
  (range "SC*")
  ;; extracted concentrations will be those in the elements
  ;; which are being extracted
  (setcomp-internal)
  ;; table of time versus instantaneous gas flow rate (kg/s)
  ;; equal to total vapor flux extracted for the well
  (table
    0.0           0.0
    23.99M        0.0
    24M          -3.95361
    24.50000M    -3.95361
    25.50000M    -34.13112
    26.50000M    -70.74704
    27.50000M    -72.10555
    28.50000M   -106.12056
    29.50000M    -79.81771
    30.50000M    -88.09417
    31.50000M    -94.88673
    32.50000M    -84.33215
    33.50000M     -7.51709
    34.50000M    -60.74632
    35.50000M    -46.08485
    36.50000M    -77.59765
    37.50000M    -85.69066
    38.50000M    -71.06054
    39.50000M   -100.32077
    40.50000M    -48.76704
    41.50000M   -102.14605
    42.50000M   -149.01988
    44M         -149.01988
    )
  )

;; infiltration flux of water
(compflux
```

```
    ;; name of source term set
    (name atmflux)
    ;; name of component being injected
    (comp water)
    ;; multiply fluxes given in table below by flow area
    ;; perpendicular to z direction
    (mult-by-area z)
    ;; range of elements at the ground surface
    (range "*#*:*:29")
    ;; flux of water (kg/s) per unit ground surface area
    ;; Avg. infiltration assumed = 10% of pptn.= 1.33 in/yr
    (table 0.0 5.35e-7  1.e30 5.35e-7)
    ) ;; end compflux

  ) ;; end srctab

;; initial conditions

;; read initial soil concentrations (kg TCE/kg total soil) from file;
;; format of the file is
;; $X.TCE
;; <i> <j> <k>  <conc>
;; <i> <j> <k>  <conc>
;; ....
;; model will internally convert from TCE soil concentrations to
;; TCE aqueous mole fractions
(read-soil-conc  (TCE "soilTCE.in"))

;; set other initial conditions
(state
  ;; table of liquid saturation vs. z, obtained from steady-state run
  (S.liquid by-ztable
    (
    2.0000e+00 1.0000e+00
    5.5000e+00 1.0000e+00
    8.0000e+00 1.0000e+00
    9.5000e+00 9.6433e-01
    1.0500e+01 6.9470e-01
    1.1750e+01 6.4265e-01
    1.3500e+01 6.0098e-01
    1.5670e+01 5.8839e-01
    1.8010e+01 5.8476e-01
    2.0350e+01 5.8266e-01
    2.2690e+01 5.8148e-01
    2.4860e+01 5.8085e-01
    2.6610e+01 5.8053e-01
    2.7860e+01 5.8037e-01
    2.8848e+01 5.8028e-01
```

```
  2.9824e+01 5.8021e-01
  3.0800e+01 5.8016e-01
  3.1776e+01 5.8013e-01
  3.2752e+01 5.8010e-01
  3.3758e+01 5.8008e-01
  3.4794e+01 5.8006e-01
  3.5830e+01 5.8005e-01
  3.6866e+01 5.8004e-01
  3.7902e+01 5.8003e-01
  3.8938e+01 5.8003e-01
  3.9974e+01 5.8003e-01
  4.1010e+01 5.8002e-01
  4.2046e+01 5.8002e-01
  4.3082e+01 5.8002e-01
  4.4600e+01 0.0000e+00
  ))

;; table of pressure vs. z, obtained from steady-state run
(P by-ztable
  (
  2.0000e+00 1.7350e+05
  5.5000e+00 1.3918e+05
  8.0000e+00 1.1467e+05
  9.5000e+00 1.0042e+05
  1.0500e+01 1.0041e+05
  1.1750e+01 1.0039e+05
  1.3500e+01 1.0037e+05
  1.5670e+01 1.0035e+05
  1.8010e+01 1.0032e+05
  2.0350e+01 1.0029e+05
  2.2690e+01 1.0026e+05
  2.4860e+01 1.0024e+05
  2.6610e+01 1.0021e+05
  2.7860e+01 1.0020e+05
  2.8848e+01 1.0019e+05
  2.9824e+01 1.0018e+05
  3.0800e+01 1.0016e+05
  3.1776e+01 1.0015e+05
  3.2752e+01 1.0014e+05
  3.3758e+01 1.0013e+05
  3.4794e+01 1.0012e+05
  3.5830e+01 1.0010e+05
  3.6866e+01 1.0009e+05
  3.7902e+01 1.0008e+05
  3.8938e+01 1.0007e+05
  3.9974e+01 1.0006e+05
  4.1010e+01 1.0004e+05
  4.2046e+01 1.0003e+05
```

```
    4.3082e+01 1.0002e+05
    4.4600e+01 1.0000e+05
    ))

  (S.liquid by-key ("IN*" 0.0))
  ;; note values in atmosphere cells will be overwritten by
  ;; values set in bctab above
  (C.air by-key ("*" 1.014e-06) ("T*" 0.995)
    ("W#*:*:1" 1.e-8) ("W#*:*:2" 1.e-8) ("IN*" 0.99))

  (S.liquid by-key ("T*" 0.0))
  ;; following will be overwritten by values read from
  ;; the soil concentration file
  (C.TCE by-key ("*" 0.0))

  ) ;; end state

;;mesh generation input
(genmsh
  (coord cylind)   ;; cylindrical mesh (r,theta,z)
  (down 0. 0. -1.) ;; positive z is upwards so down vector is (0,0,-1)
  ;; r subdivisions (m)
  (dx 0.065 4*0.5 0.7 1.0 1.5 1.7 2.0 3.0 5 7 2*10 15 2*20)
  ;; theta subdivision (degrees)
  (dy 360)
  ;; z subdivisions (m)
  (dz
    4.0 3.0 2.0 1.0 1.0 1.5 2.0 4*2.34 2.0 1.5 1.0
    5*0.976    10*1.036    0.01
  ) ;; end dz

  ;; element prefix names and material types
  (mat
    (W  san1  1 nx  1 1   1  4)
    (C  san1  1 nx  1 1   5 nz)
    (T  ATM   2 nx  1 1  nz nz)
    (IN WEL   1  1  1 1   5 30)
    (SC SCR   1  1  1 1  15 19)
    (B  san1 nx nx  1 1   1 29)
    ) ;; end mat

  ) ;; end genmsh

) ;;; end usnt
```